Precipitation of Nb in Ferrite After Austenite Conditioning. Part II: Strengthening Contribution in High-Strength Low-Alloy (HSLA) Steels

M.A. ALTUNA, AMAIA IZA-MENDIA, and I. GUTIÉRREZ

Often, Nb contributes to the strength of a microalloyed steel beyond the expected level because of the grain size strengthening resulting from thermomechanical processing. Two different mechanisms are behind this phenomenon, and both of them have to do with the amount of Nb remaining in solution after hot rolling. The first of them is the increase of the hardenability of the steel as a result of Nb, and the second one is the fine precipitation of NbC in ferrite. Three Nb microalloyed steels were thermomechanically processed in the laboratory and coiled at different temperatures to investigate the effect of Nb content on the tensile properties. The extra strength was linearly related to the Nb remaining in solution after the hot working. The maximum contribution from Nb was reached for a coiling temperature of 873 K (600 °C).

I. INTRODUCTION

THERMOMECHANICAL processing of Nb microalloyed steels produces improved mechanical properties when compared with C-Mn steels of similar composition. The two possible main strategies during hot rolling are conventional control rolling and recrystallization control rolling.[1,2] In conventional rolling, the aim is to accumulate some strain in the austenite to enhance the number of nucleation sites for ferrite formation. In recrystallization control rolling, the aim is to limit grain coarsening during interpass times. Nb acts on the austenite microstructure through the solute drag effect, but it is used mainly for its ability to produce strain-induced precipitation within the relevant temperature interval that induces strain accumulation in austenite before transformation. However, it is expected that sheet rolling involving a fast process with short interpass times at a finishing mill (~10 seconds) will not allow full precipitation of Nb before cooling. The Nb remaining in solution can affect the final microstructure and its mechanical behavior, and it is usual to obtain some extra strengthening that cannot be accounted for by the ferrite grain size and the solutes.

The contributions from different strengthening mechanisms to the yield stress of a low-carbon microalloyed steel can be considered additive,[3] leading to the following equation:

$$\sigma_y = \sigma_0 + \sigma_{ss} + k \cdot d^{-1/2} + \sigma_p + \sigma_\rho + \sigma_{ppt} \quad [1]$$

where d is the average grain size (mean linear intercept) of the ferrite and k is in 15 to 18 (MPa mm$^{0.5}$) range;[4] σ_p, σ_ρ, and σ_{ppt} are the contributions from pearlite, dislocations and precipitation, respectively; σ_0 is the ferrite lattice friction stress, and σ_{ss} is the contribution from the elements in solid solution.

The contribution from a given solute is generally expressed as being proportional to its weight percent.[4] A linear relation has also been found for Nb, and early data from Morrison[5] gave for Nb a mean value of 1500 MPa/wt pct with an upper bound at 3000 MPa/wt pct. Nb is a strong carbonitride-forming element that can precipitate at different stages during thermomechanical processing: (1) during hot rolling interpass times, (2) in austenite during the cooling after finishing rolling, (3) at the transformation interphase, and (4) homogeneously in ferrite or alternatively, it can remain in solution. This produces an important variability in terms of the expected contribution attributable to Nb and is the cause of the large scatter on the proportionality constant.[5] In a more recent work, a proportionality between the tensile strength increase and the Nb$_{free}$, available to precipitate in ferrite has also been deduced, leading to a value of 2220 MPa per weight percent.[6]

The Nb$_{free}$ concentration depends on the processing conditions, cooling rate, and transformation temperature.[6] A cooling rate higher than a critical value is needed to keep Nb in totally solution and get the maximum precipitation strengthening (general precipitation in ferrite). If the cooling rate is below this critical value, then the precipitation happens totally or partially in austenite, consumes Nb, and reduces the potential precipitation strengthening. This critical cooling rate has to be related to the steel chemistry and to the transformation temperature.[6] When Nb is left in solution, its contribution to the strength (and in particular the

M.A. ALTUNA, Metallurgy Engineer, formerly with the Materials Department, CEIT, Manuel de Lardizabal, 15, 20018 San Sebastián, Spain, is now with Grupo WEC, Polígono Industrial no 38, Parcela N1-1, 20829 Itziar Deba, Gipuzkoa, Spain. AMAIA IZA-MENDIA, Researcher, and I. GUTIÉRREZ, Senior Researcher, are with the Thermomechanical Treatments Group, Materials Department, CEIT and Tecnun (University of Navarra), Manuel de Lardizabal 15, 20018 San Sebastián, Spain. Contact e-mail: aiza@ceit.es
Manuscript submitted November 11, 2011.
Article published online October 2, 2012.

Table I. Recompilation of Representative Literature Results Including Steel Composition, Processing Conditions, Type of Precipitates, and Strengthening Contribution

Steel	Thermomechanical Sequence	Cooling Conditions	Precipitation	x (nm)	$\Delta\sigma_y$ (MPa)	Ref.
0.07C 0.98Mn 0.043Nb	Industrial: reheating: 1423 K (1150 °C) Finish rolling: 1353 K to 1163 K (1080 °C to 890 °C)	10 K/s to 923 K (650 °C)	γ and interphase precipitation on a coarse scale	NA	58 (Negligible contribution from dislocations)	7
0.08C 1Mn 0.065Nb	Industrial: reheating: 1463 K (1190 °C) Roughing exit: 1323 K (1050 °C) Finishing T: 1203 K to 1143 K (930 °C to 870 °C)	Laminar water wall and coiling at 923 K (650 °C)	In austenite	10 to 50 nm if FT = 1143 K (870 °C) 5 to 20 nm if FT = 1203 K (930 °C)	~65	8
0.07C 0.33Mn 0.02Nb	Experimental hot rolling mill Reheating: 1473 K (1200 °C) Roughing: 1413 K to 1303 K (1140 °C to 1030 °C)	50 K/s to 953 K (680 °C) 0, 2, 5 h at 953 K (680 °C)	γ grain boundaries Nb remaining in solution: 0.01 pct	7.2 at 0 h 5.2 at 2 h	-	9
		Continuous cooling	γ grain boundaries and matrix, interphase precipitation α matrix	~6.5 nm	-	
0.07C 1.1Mn 0.025Nb	Finishing: 1201 K to 1165 K (928 °C to 892 °C)	50 K/s to 953 K (680 °C), 0, 2, 5 h at 953 K (680 °C)	γ grain boundaries Nb remaining in solution: 0.016 pct	5.6 for 0 h 3.9 for 5 h at 953 K (680 °C)	—	
		Continuous cooling	γ grain boundaries and matrix, γ deformation bands interphase precipitation α matrix	6.3 to 3.0 nm 5.0 nm 3 nm	—	
0.17C 1.3Mn 0.13Nb	Solution treated at 1523 K (1250 °C), oil quenched, reaustenized to the same temperature	Salt bath at temperatures from 873 K to 973 K (600 °C to 700 °C) and WQ to RT	Mainly interphase precipitation	3.3 to 6.2	Estimated from HV. 200 to 390	10
0.055C 0.55Mn 0.02Nb 0.06Ti	Industrial reheating: 1503 K (1230 °C) Roughing end: 1433 K (1160 °C) Finishing: 1373 K to 1143 K (1100 °C to 870 °C)	20 K/s to 903 K (630 °C) Cooling rate in the coil > 30 K/h	~50 pct of Nb+Ti remain undissolved after reheating ~27 pct of Nb+Ti precipitated in austenite ~23 pct of Nb+Ti (~0.005Nb and 0.013Ti) remained in solution after coiling No interphase precipitation	67 6.8	78	11

Table I. continued

Steel	Thermomechanical Sequence	Cooling Conditions	Precipitation	x (nm)	$\Delta\sigma_y$ (MPa)	Ref.
0.11C 1.54Mn 0.04Nb0.11Ti	Industrial: reheating: 1498 K (1225 °C), Roughing: >1373 K (1100 °C), Finishing: 1168 K (895 °C)	10 K/s to 923 K (650 °C)	~50 pct of grains with precipitation in γ ~50 pct of the grains with interphase precipitation	7.2 4.0	Estimated from TEM 92 precipitation in γ 112 interphase precipitaiton 64 dislocations	12

FT, finishing temperature; *NA*, not available; *RT*, room temperature; *TEM*, transmission-electron microscopy; *WQ*, water quenching.

precipitation strengthening) is highly dependent on the coiling temperature.

An extremely important amount of work has been dedicated to investigating the effects of Nb on the development of the austenite microstructure and on how this affects phase transformation. The available results dealing with the evolution of Nb after hot deformation are scarce. Nevertheless, a series of source studies is regularly cited,[7–12] and some of them have been compiled in Table I.

Based on these results, it is claimed that under industrial conditions, it is not possible to obtain a significant contribution from homogeneous precipitation of Nb in ferrite. Some of the industrially processed steels in Table I refer to Nb and Ti microalloyed steels, which present a complex precipitation pattern that combines some of the following phenomena: incomplete solutioning, partial precipitation in austenite, partial interphase precipitation, and some Nb + Ti remaining in solution for a coiling temperature of 903 K to 923 K (630 °C to 650 °C).[11,12] The industrially processed Nb microalloyed steels were reheated at a relatively low reheating temperatures and were processed in such a way that most of the precipitation took place in austenite or at a coarse scale at the interphase for a coiling temperature of 923 K (650 °C), which produced a ferrite-pearlite microstructure with an extra strengthening of 58 to 65 MPa.[7,8] In the group of the laboratory-processed steels, those with a ~0.02Nb content showed that relatively fine precipitates formed in austenite and apparently no further precipitation occurred in ferrite for a coiling temperature of 953 K (680 °C), followed by air cooling to room temperature.[9] The result was that approximately 0.010 to 0.016 Nb remained in solution. When continuous air cooling to room temperature was applied, the A_{r3} was 1110 K and 1063 K (837 °C and 790 °C) for low and high Mn content, respectively, and different families of Nb-rich precipitates were detected (Table I).[9]

The presence of Nb in solution before transformation increases the hardenability of the steel, and frequently, quasi-polygonal and non-polygonal ferrite microstructures are obtained in Nb-microalloyed steels under cooling conditions that would produce equiaxed ferrite in C-Mn steels. The displacive type of transformation that produces nonpolygonal ferrite or bainite leads to highly dislocated substructures.[13–15] The dislocation density in bainite and martensites can be expressed by an empirical relationship that is valid over the temperature range 570 K to 920 K (297 °C to 647 °C), covering martensite, bainite, and Widmanstätten ferrite[16]

$$\log \rho = 9.28480 + \frac{6780}{T} - \frac{1,780,360}{T^2} \quad (\rho \text{ in m}^2 \text{ and } T \text{ in K})$$

[2]

where T is the transformation temperature.

The expected contribution of the dislocation density in Eq. [1] can be expressed by

$$\sigma_\rho = \alpha M \mu \boldsymbol{b} \sqrt{\rho}$$

[3]

Table II. Chemical Steel Composition (wt pct)

Steel	C	Si	Mn	Al	Nb	V	N
A	0.06	0.35	1.00	0.047	0.056	—	0.0059
B	0.15	0.30	1.42	0.037	0.033	0.011	0.007
C	0.13	0.02	1.20	0.045	0.02	—	0.037

where α is a numerical factor, M is the Taylor factor, μ the shear modulus, and b is the magnitude of the Burgers vector. The actual contribution from the dislocations depends on the value assigned to αM. A value of $\alpha M = 0.4$ has been taken into consideration for iron.[7] Alternatively, an empirical equation can be used[17]

$$\sigma_\rho \,(\text{MPa}) = 1.3(600 - T) \qquad [4]$$

where T the transformation temperature in °C.

A value of $\alpha = 0.2$ seems to make these two formulations reasonably compatible.[18] For a Nb microalloyed steel industrially coiled at 923 K (650 °C), a dislocation density of 10^8 cm^{-2} was determined,[7] with a negligible contribution to the yield strength. In contrast, when applying in the laboratory an accelerated cooling (50 K/s) to 953 K (680 °C) dislocation densities as high as 6 to 16 $\times$ 10^{13} m^{-2} where reported, whereas air cooling to room temperature (A_{r3} = 1110 K or 1063 K [837 °C or 790 °C]) produced densities of 4 to 5 $\times$ 10^{13} m^{-2}.[9] According to the preceding equations, these relatively high dislocation densities would significantly contribute to the mechanical properties.

The precipitation strengthening found in Nb-microalloyed steels is usually well described by Ashby-Orowan's equation[3,19,20]

$$\sigma_{\text{ppt}} \,(\text{MPa}) = 10.8 \frac{\sqrt{f_v}}{x} \ln \frac{x}{6.125 \times 10^{-4}} \qquad [5]$$

where f_v is the volume fraction of the particles and x is the average precipitate diameter in micrometers. This equation, which applies to nonshearable particles, shows remarkable agreement when applied to low-carbon microalloyed steels.[19] For shearable precipitates, the dislocations cut through the particles and the corresponding shear stress becomes a function of the critical force to break the particle F.[21] The strengthening becomes highly dependent on the detailed interaction mechanisms between the dislocations and the obstacles (precipitates), and F becomes proportional to the particle size.[22] The result is that, independently of the interaction mechanism, for shearable particles, the critical resolved shear stress decreases for decreasing particle size.

It was shown previously[23,24] that, depending on the coiling temperature applied to a 0.06C-1Mn-0.056Nb steel, different microstructures ranging from ferrite-pearlite to mixed microstructures can be produced. Some precipitation was also observed in ferrite. The current work is the second of a series of two that has gone in depth into this subject. The first part[25] was dedicated to investigating the ferrite microstructure obtained at high coiling temperatures by transmission electron microscopy. The ferrite, formed for a coiling temperature ranging between 873 K and 1023 K (600 °C and 750 °C), did not show significant differences in dislocation density, image quality maps, or grain boundary distribution. Both heterogeneous AlN precipitation at dislocation and discontinuous interphase Nb precipitation were observed for the coiling at 1023 K (750 °C). Coiling at 873 K (600 °C) produced a faster transformation to ferrite than at 1023 K (750 °C), as well as a heterogeneous distribution of very fine Nb precipitates that followed the Baker-Nutting orientation relationship with ferrite. These precipitates were very stable when prolonging the holding time at 873 K (600 °C) up to 48 hours. In this second part, we turn our attention to analyzing the effect on the mechanical properties, the effect of the processing conditions, and the steel composition, relating them to the microstructure and precipitation.

II. EXPERIMENTAL PROCEDURE

Three Nb-microalloyed steels are considered in the current work. The composition of the steels is shown in Table II. Steel A is the same one used in the first part of this study.[25]

Plane strain compression tests were performed on industrially produced wrought steels to condition the austenite and investigate the effect of the coiling conditions. The load was applied on the initial rolling plane and perpendicular to the rolling direction. The applied thermomechanical sequences are detailed in Section III.

Tensile specimens were machined out from the central part of the plane strain compression specimens with the axis parallel to the longitudinal direction (former rolling direction). The tensile tests were performed at room temperature, with a strain rate of 10^{-3} s^{-1} on a 4505 Instron testing machine (Instron Corporation, Norwood, MA) under strain control. The 0.2 pct proof stress and the ultimate tensile strength have been determined as a mean of at least two tests. A selection of steel A specimens was also tested in tension at temperatures in the range of 423 K to 623 K (150 °C to 350 °C) to investigate dynamic strain aging.

Specimens for optical microscopy were obtained from the plane strain compressed specimens at approximately the same location as the tensile specimen gage length. At small applied strains (i.e., $\varepsilon = 0.3$), the tensile specimen section is smaller than the thickness of the deformed zone in compression. The mean grain size estimated over this region and that throughout the entire compressed section[23] can be significantly different. As the total applied strain increases, the difference reduces.

The surface of the specimens was prepared by standard metallographic techniques and a final etching in 2 pct Nital. The ferrite grain size (mean linear intercept) and the pearlite volume fraction were determined by quantitative metallography techniques.[26]

III. THERMOMECHANICAL SEQUENCES

To define the thermomechanical schedules for the plane strain compression test, the MOFIPRE model[27] was used because it allows the recrystallization and the precipitation kinetics in austenite and the interactions between these two phenomena to be calculated. The deformation sequences applied to steels A, B, and C were slightly different.

Steels A and C were reheated at 1523 K (1250 °C) and steel B at 1473 K (1200 °C). The holding time was 15 minutes for steels A and C and 20 minutes for steel B, followed by cooling at ~3 K/s to the deformation temperature. The following thermomechanical sequences were applied:

- One-pass deformation sequence (S1): Deformation at 1373 K (1100 °C) and 1 s^{-1} to a strain of $\varepsilon = 0.3$ for steel A and $\varepsilon = 0.5$ for steel B. For steel C, deformation was performed at 1323 K (1050 °C) and 1 s^{-1} to a strain of $\varepsilon = 0.3$. After deformation, a holding stage of 20 seconds was applied at the same temperature to assure the recrystallization of the austenite before cooling. According to the model predictions, these conditions are outside the range required for Nb carbonitride precipitation in austenite. For steel B, some Nb remains out of solution after the reheating (~0.012 pct).
- Two-pass deformation sequence (S2) is aimed at accumulating strain in austenite before transformation. The first pass was performed under the same conditions applied to the one-pass sequence, then cooling was carried out to the second deformation pass temperature: 1273 K (1000 °C) for steel A and 1223 K (950 °C) for steel B. The second pass deformation was performed at a strain rate of 1 s^{-1} and the deformation per pass was of $\varepsilon = 0.3$ for the two steels. This sequence was not applied to steel C.

After both S1 and S2 deformation sequences, the following different cooling schedules were applied:

- Coiling: The specimens were cooled to coiling temperature at approximately 5 K/s for steel A and 10 K/s for steel C. For steel B, a cooling rate of approximately 5 K/s was applied, and in addition, a rate of 15 K/s (fast cooling [FC]) was also applied before coiling at 673 K and 573 K (400 °C and 300 °C). Coiling was simulated by holding for 1 hour followed by slow cooling into the furnace (~35 K/h) to room temperature. Coiling temperatures in the range 573 K to 1023 K (300 °C to 750 °C) were applied.
- Reference test (S1-R and S2-R): After the one- or two-pass deformation sequence (S1 or S2) described

previously, the specimen was cooled at a rate of approximately 3 K/s to 1143 K (870 °C) and held at this temperature for 1 hour. This was applied only to steels A and C and for a coiling temperature of 923 K (650 °C). The strain-induced precipitation model predicts the full precipitation of the Nb as a result of this holding stage for steel A when processed according to the S2-R sequence.[25] Nevertheless, no precipitation is expected in steel C after the S1-R.
- Prolonged holding at coiling temperature: The same conditions applied to coiling were applied, except that the holding time was 6, 24, or 48 hours, instead of the 1 hour applied to the coiling simulations. This was only applied to steel A.

IV. RESULTS

Ferrite-pearlite microstructures are obtained in steel A for coiling temperatures equal to or higher than 873 K (600 °C), leading to a pearlite volume fraction of approximately 5 pct. Examples of these microstructures are shown in Part 1,[25] whereas Figure 1 shows SEM images of the samples processed according to S1 and S2 and coiled at 873 K (600 °C). Decreasing the coiling temperature leads to mixtures of polygonal ferrite and bainitic microstructures, as can be observed in Figure 2.

The microstructures obtained in steel B are shown in Figure 3 (optical images) and in Figure 4 (SEM images), as a function of the coiling temperature. In this steel, coiling at 873 K (600 °C) produces a significant fraction of acicular components, whereas at 923 K (650 °C), a ferrite-pearlite microstructure develops. The pearlite volume fraction ranges between 21 pct and 26 pct for these microstructures. The decrease of the coiling temperature increases the fraction of bainite in the final microstructure and coiling at 573 K (300 °C) leads to the formation of a fully bainitic microstructure. It is clear that the S2 sequence has a refining effect, independently of the final microstructure and steel composition.

The optical and SEM micrographs in Figure 5 correspond to steel C coiled at 993 K and 923 K (720 °C and 650 °C). The microstructures are mainly composed of ferrite, pearlite, and some acicular ferrite. The plates of acicular ferrite seem to be associated to the pearlite regions. The volume fraction of pearlite is of approximately 23 pct and 29 pct, respectively, for coiling at 923 K and 993 K (650 °C and 720 °C). The microstructure appears banded for coiling at 993 K (720 °C), but this effect is not so apparent for the specimen coiled at 923 K (650 °C).

The mean ferrite grain size for the F + P microstructures for all three steels has been plotted in Figure 6 as a function of the coiling temperature. The grain refinement produced with the S2 sequence is clear. Decreasing the coiling temperature for steels A has a refining effect after the S1 sequence. For the S2 sequence, the ferrite grain size is almost independent on the coiling temperature. Holding for 1 hour at 1143 K (870 °C) before
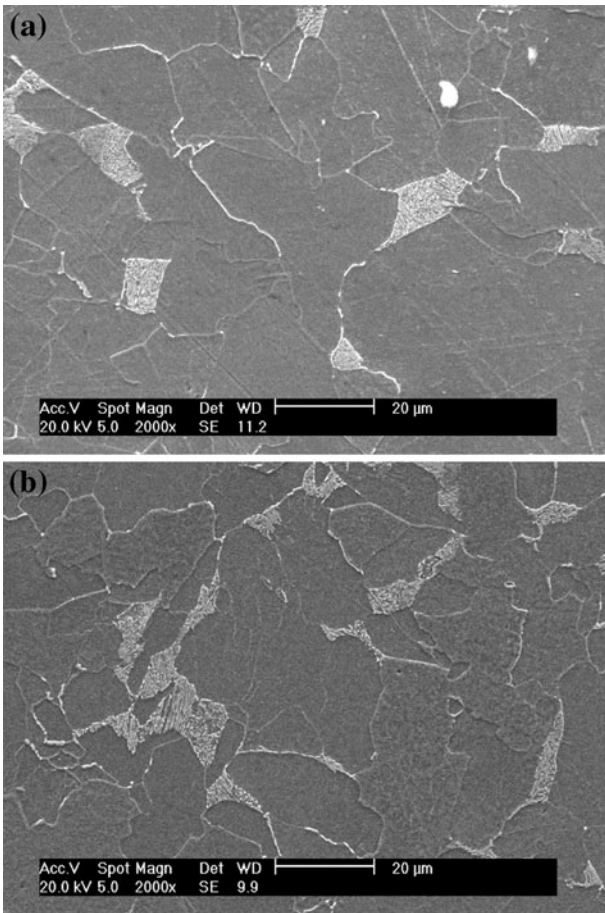
Fig. 1—Steel A. Ferrite pearlite microstructures obtained with sequences (*a*) S1 and (*b*) S2 and a coiling temperature of 873 K (600 °C).

Fig. 2—Steel A. Optical micrographs showing mixed microstructures produced after sequence S1 when coiling at a low temperature (*a*) 823 K (550 °C) and (*b*) 623 K (350 °C).

coiling (reference tests) does not modify the grain size produced with the one-pass deformation sequence (S1). However, the same holding stage counteracts to some extent the refining effect of the two-pass deformation sequence (S2). The coarsest mean grain size in steel B produced with the S1 sequence almost coincides with the size after the S2 sequence in steel A. The one-pass deformation sequence applied to steel C developed a coarse ferrite grain size, which is almost independent of the coiling temperature within the investigated range.

The variation of the tensile properties with the applied sequence and the coiling temperatures is shown in Figure 7 for the three steels. After sequence S1, steels A and B produce similar mechanical properties for the same coiling temperature. Nevertheless, after sequence S2, steel B consistently produces higher tensile properties than steel A. Steel C is softer than steel A and B. For the upper coiling temperature range (≥ 873 K [600 °C]), a monotonic increase of both the yield and tensile strength, which can reach 100 to 120 MPa, is observed with decreasing coiling temperatures. Lowering the coiling temperature (below ~873 K [600 °C]) produces a slight decrease or some stagnation of the tensile properties, except when a fully bainitic microstructure is produced, in which case, the values increase over those
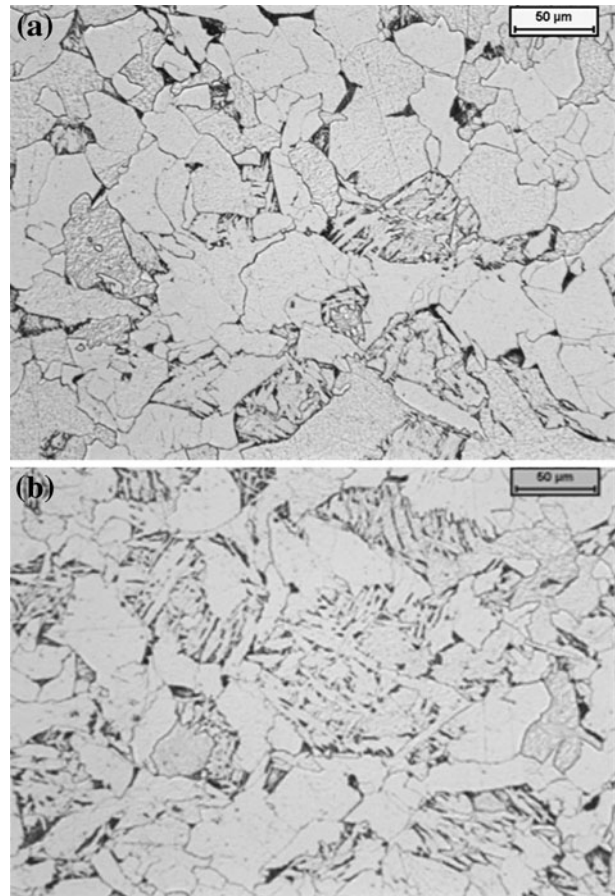
for ferrite-pearlite. A good example of this is the steel B cooled at ~15 °C/s to the coiling temperature of 673 K or 573 K (400 °C or 300 °C) (FC).

The S1-R sequence produces an unstable condition for steel A. tensile specimens machined from different plane strain compression tests produce a much broader scatter than for any other sequence. This variability can be attributed to the delayed Nb precipitation in a recrystallized austenite. The applied model predicts the completion of Nb precipitation after ~1 hour holding at 1143 K (870 °C), but this can vary depending on local Nb concentration and/or small deviations in processing conditions.[25] This is why the tensile results for S1 have not been plotted in Figure 7. Nevertheless, independently of the previous deformation sequence and of the scatter in yield strength for S1, the steel is softer when it is held at 1143 K (870 °C) before coiling at 923 K (650 °C).

Free nitrogen can make a significant contribution to the tensile properties. To investigate the effect of the coiling temperature on the amount of free nitrogen, some selected steel A specimens from S1 were submitted to internal friction tests. Unfortunately, no conclusive results were obtained. As an alternative, dynamic strain aging was investigated by performing tensile tests at
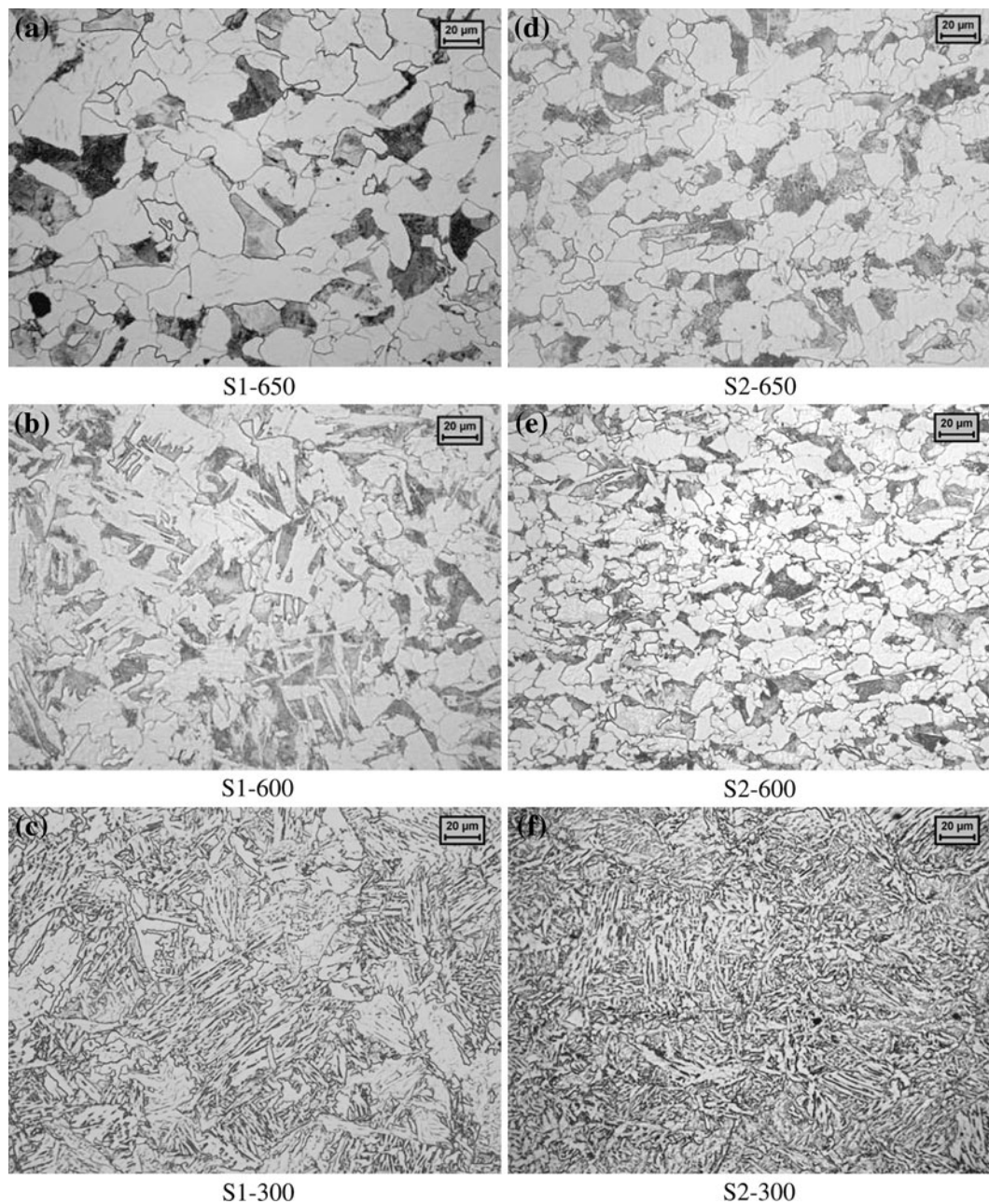
Fig. 3—Optical micrographs showing the microstructures obtained in steel B for different deformation sequences and coiling temperatures. Sequence S1 and coiling at (*a*) 923 K (650 °C), (*b*) 873 K (600 °C), and (*c*) 573 K (300 °C). Sequence S2 and coiling at (*d*) 923 K (650 °C), (*e*) 873 K (600 °C), and (*f*) 573 K (300 °C).

different temperatures. The graph in Figure 8 shows some examples of the tensile curves obtained at room temperature, 473 K and 623 K (200 °C and 350 °C) with steel A thermomechanically processed according to the S1 sequence but different coiling temperatures. Some oscillations can be observed on the curves obtained at 473 K and 623 K (200 °C and 350 °C), whereas those produced at room temperature are smooth. Deformation at 473 K (200 °C) leads to lower yield and tensile strengths and a higher elongation than at room temperature, but steel ductility decreases for the test performed at 623 K (350 °C), independently of the coiling

temperature. The dependence of the tensile strength with respect to the tensile test temperature is shown in Figure 9. It can be observed that for coiling at 1023 K, 973 K, and 673 K (750 °C, 700 °C, and 400 °C), the tensile strength decreases monotonously with an increase in the tensile test temperature in the range of 293 K to 623 K (20 °C to 350 °C). Coiling at 873 K (600 °C) produces a singular behavior: When increasing the tensile test temperature in the range from 293 K to 473 K (20 °C to 200 °C), the tensile strength decreases, but between 473 K and 623 K (200 °C and 350 °C), the tensile strength increases.
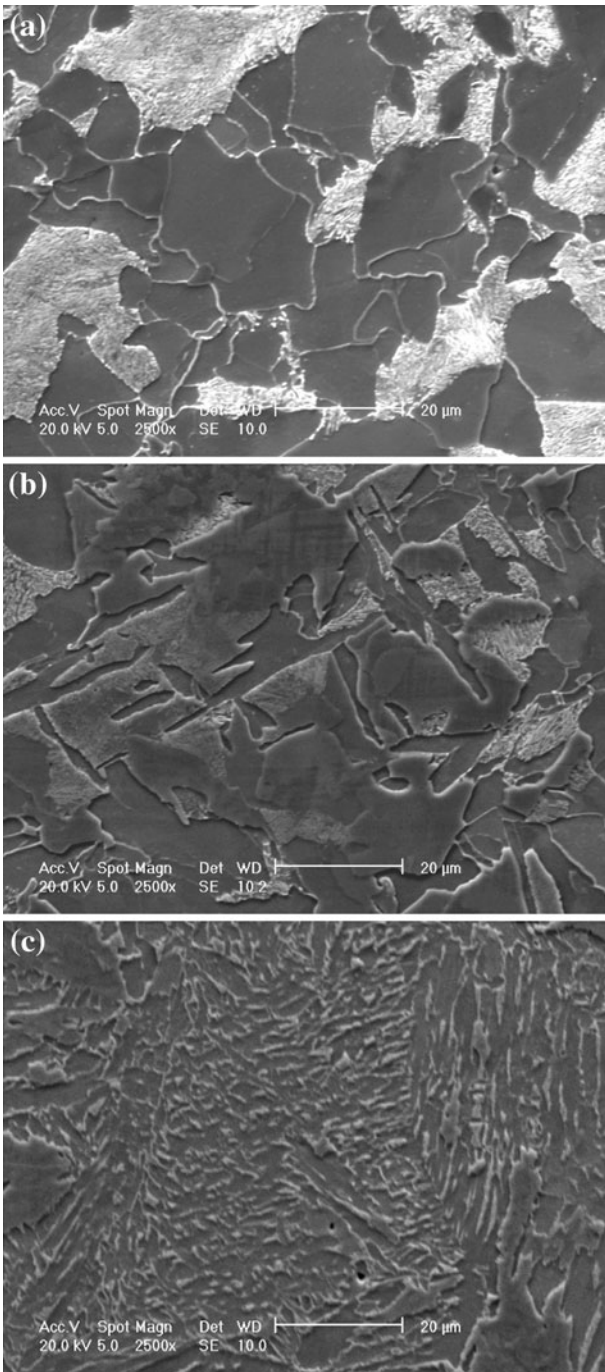
Fig. 4—SEM images showing some details of the microstructures obtained in steel B with sequence S1 and different coiling temperatures: (*a*) 923 K (650 °C), (*b*) 873 K (600 °C), and (*c*) 573 K (300 °C).

V. DISCUSSION

The applied deformation sequences were designed *via* modeling[27] to condition the austenite in two different ways. Sequence 1 (S1) was aimed at producing a recrystallized austenite, whereas sequence 2 (S2) resulted in some strain accumulation in austenite before transformation. S1 produced a ferrite-pearlite microstructure in steel A for coiling temperatures equal to or higher than 873 K (600 °C) (Figure 1). Within this temperature range, the final ferrite grain size increased with the coiling temperature, as shown in Figure 6. The reason for this dependency can be understood in terms of two different but overlapping mechanisms. First, transformation under a low undercooling below A_{r3} results in low driving energy for nucleation that leads to reduced density of ferrite nuclei. The second factor is the ferrite coarsening taking place behind the transformation front.[28,29] Consequently, it seems logical that coiling at 873 K (600 °C) produces a finer grain size than coiling at 1023 K (750 °C). In this same steel, S2 produces a significant grain refinement with respect to S1, leading to a mean grain size of approximately 14 μm, which remains almost constant over the 873 K to 1023 K (600 °C to 750 °C) range of coiling temperatures. The strain accumulated in austenite increases the density of the ferrite nuclei. This together with the fact that the ferrite grain coarsening is to some extent reduced when strain accumulates in austenite explains the lesser influence of the coiling temperature on the final grain size for S2. The coalescence mechanism, which is one of the main mechanisms of the ferrite grain coarsening behind the transformation front, occurs between ferrite grains separated by low misorientation boundaries, but the density of such boundaries reduces when the transformation happens from a deformed austenite.[30]

The higher carbon content in steel B, as compared with steel A, produces a higher volume fraction of pearlite and increases hardenability; this last effect is manifested by a greater tendency to form bainitic microstructures in steel B (Figures 2, 3). Coiling at 873 K (600 °C) produces some bainite in steel B, whereas in steel A, the microstructure is ferrite-pearlite. At low coiling temperatures, a fully bainitic microstructure is obtained in steel B (Figure 4), whereas in steel A, a mixture of ferrite-pearlite and bainite is produced. Steel B, when coiled at 923 K (650 °C), gives grain sizes of 14 and 7 μm, respectively, after sequences S1 and S2, which are significantly finer than those obtained in steel A. In addition to the difference in composition that affects Ar_3, both a lower reheating temperature and a higher strain applied throughout the S1 sequence to steel B, compared with steel A, contribute to the grain size refinement. In the S2 sequence applied to steel B, the second pass deformation temperature was lower than that used to deform steel A. This difference in the thermomechanical sequence also contributes to the grain refinement observed in steel B.

In steel C, a small fraction of acicular ferrite appears together with ferrite-pearlite, even for a coiling temperature as high as 993 K (720 °C). This can be explained by the coarse austenite grain size resulting from the application of the S1 sequence to this steel. The low Nb content cannot control the austenite grain size under the applied conditions, leading to a coarser ferrite grain size than the other two steels (Figure 6). This steel is relatively soft, and the tensile properties remain almost the same after coiling at 923 K (650 °C) or at 993 K (720 °C) (Figure 7). The only specimens to show low yield stress are those corresponding to the reference test (S2-R) and to S1 and S2 after coiling at 1023 K (750 °C) for steel A.
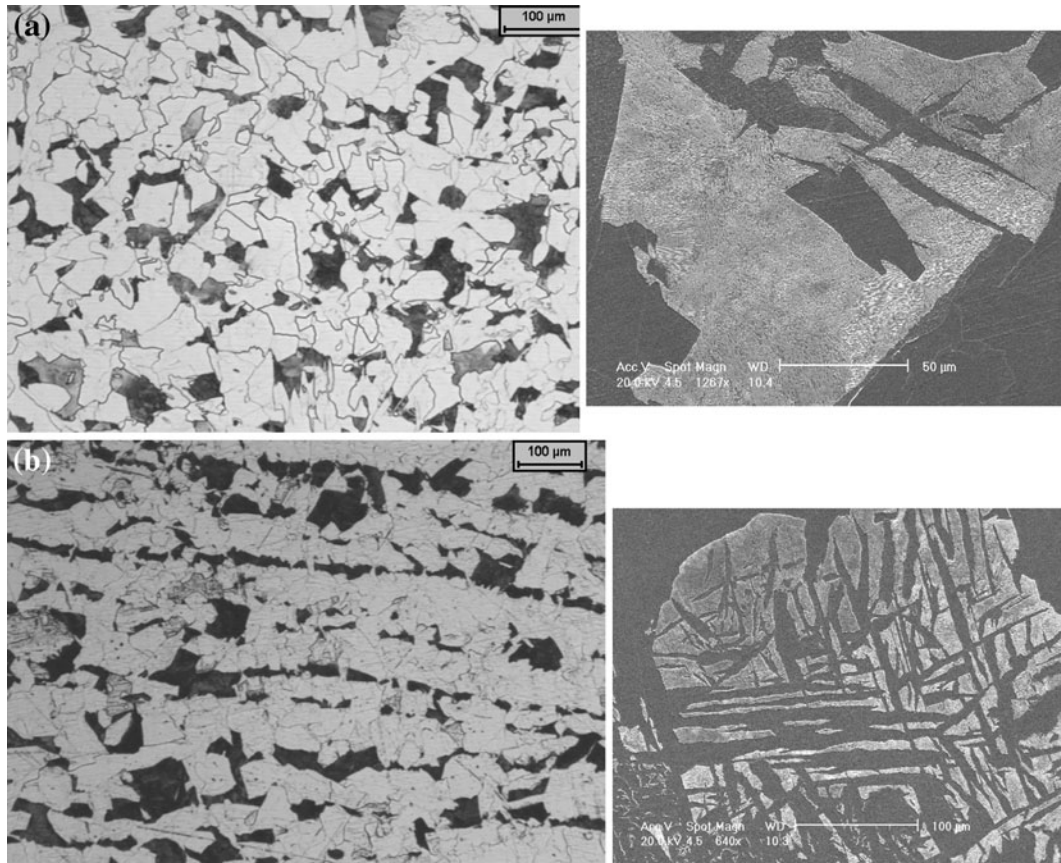
Fig. 5—Optical (left) and SEM (right) images showing the microstructure of steel C after coiling at (*a*) 923 K (650 °C) and (*b*) 993 K (720 °C).
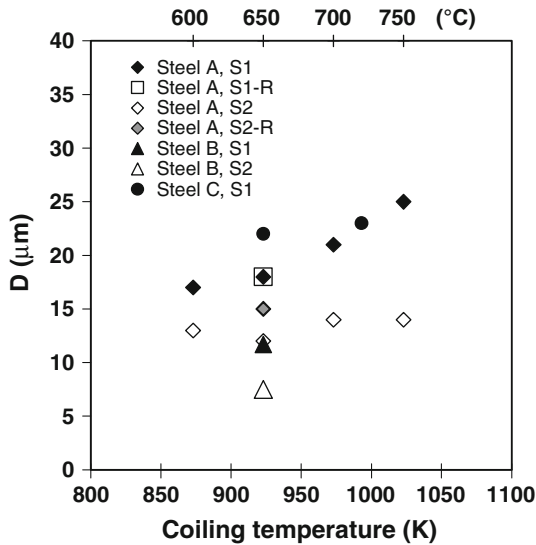

Fig. 6—Ferrite grain size as a function of the thermomechanical sequence and coiling temperature.

Fig. 7—Yield and tensile strength as a function of the coiling temperature and the thermomechanical sequence for the three steels.

A. *Yield to Tensile Strength Ratio: Microstructure and Grain Size*

The yield to tensile strength ratio has been plotted in Figure 10(a), as a function of the coiling temperature. The variation is not very pronounced among the diffe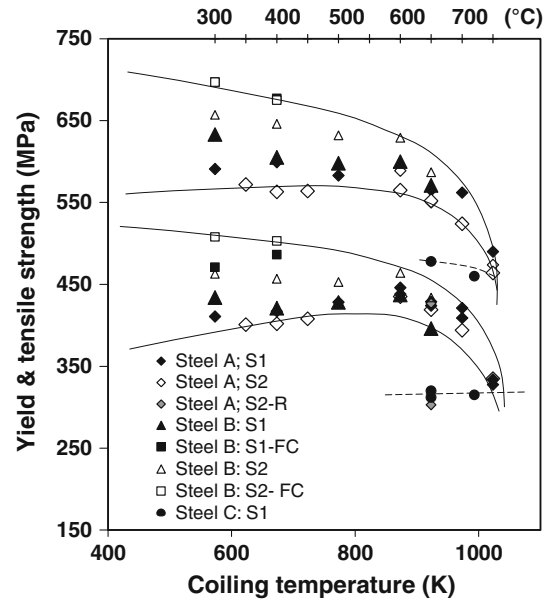rent steels and processing conditions; it varies between 0.67 and 0.77. Some lines have been drawn to approximately separate the diagram into the following regions: ferrite-bainite, bainite, and ferrite-pearlite. In the first of these regions, as the coiling temperature
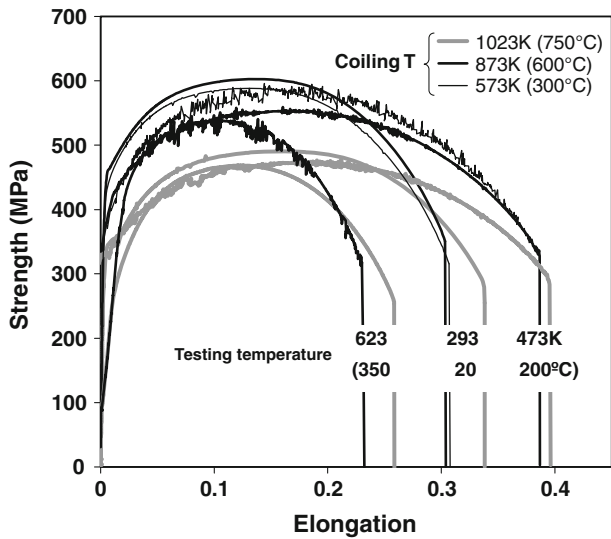
Fig. 8—Engineering tensile curves obtained at different testing temperatures with steel A thermomechanically processed according to the sequence S1 and a series of coiling temperatures.
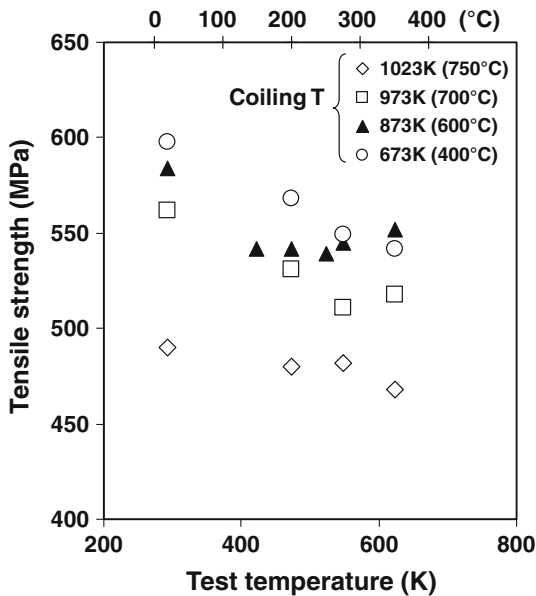

Fig. 9—Variation of the tensile strength with the tensile test temperature in steel A processed according to the sequence S1 and different coiling temperatures.
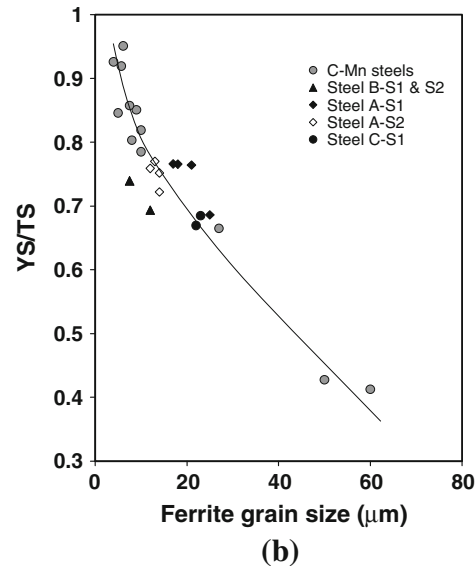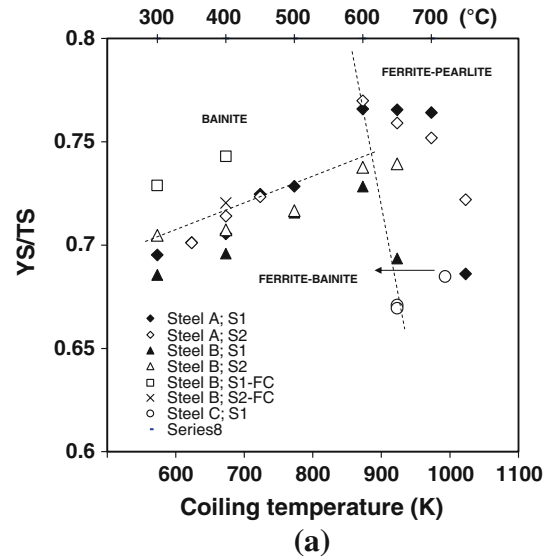

(a)

(b)

Fig. 10—Evolution of the yield/tensile strength ratio, as a function of (a) the coiling temperature and (b) for ferrite-pearlite microstructures, of the ferrite mean grain size. In this last case, the results are compared with those obtained with plain carbon mild steels.[34].

decreases (and the bainite fraction increases), the ratio slightly reduces. For fully bainitic microstructures this same trend holds, but the yield to tensile ratio becomes higher than for mixed microstructures. It seems clear that in the ferrite-pearlite region (coiling temperatures >873 K [600 °C]), the ratio YS/TS (yield to tensile strength) increases when the coiling temperature decreases. The main shift happens between 1023 K and 973 K (750 °C and 700 °C), and it affects both S1 and S2. It has to be noted that the yield point elongation almost vanishes for the steel coiled at 1023 K (750 °C), and this can explain part of this major difference in the

yield to tensile strength ratio. Nevertheless, the decrease in the ratio with the coiling temperature is the expected trend for ferrite-pearlite plain C-Mn steels because the strain hardening increases with the grain size.[31] When comparing the current results with those obtained in C-Mn steels,[34] Figure 10(b), it can be seen that the C-Mn-Nb steels follow almost the same trend as the C-Mn steels, but small deviations appear, which indicates that factors other than grain size play a role.

B. Contribution of Nb in Solution to the Yield Strength

For ferrite-pearlite microstructures, the contribution of Nb to the yield stress can be estimated by subtracting the grain size, solute, and pearlite contributions and the lattice friction stress from the experimental yield stress, $\sigma_{y\exp}$, leading to[32,33]

$$\Delta\sigma_y = \sigma_{y\,\mathrm{exp}} - \left(\sigma_0 + \sigma_{ss} + \sigma_p + 17.4d^{-1/2}\right) \qquad [6]$$

where $\sigma_o = 54$ MPa and the contribution from solutes is given by

$$\sigma_{ss} = 32\mathrm{Mn} + 678\mathrm{P} + 83\mathrm{Si} + 31\mathrm{Cu} - 31\mathrm{Cr} + 11\mathrm{Mo}$$
$$+ 5544(\mathrm{N}_{ss} + \mathrm{C}_{ss}) \qquad [7]$$

where the concentrations are expressed in wt pct, and N_{ss} and C_{ss} are nitrogen and carbon in solid solution, respectively. This equation has been recently applied[34] with some success to low-carbon steels. Here, it will be applied to determining $\Delta\sigma_y$ for the microstructures produced at high coiling temperatures for which a ferrite-pearlite microstructure is obtained.

Steels B and C have a higher carbon content than steel A, which produces a pearlite volume fraction of around 25 pct with an interlamellar spacing, $\lambda \cong 0.35$ μm. This is a relatively high pearlite content and equations other than Eq. [6] have been tested.[33] These equations produced an overestimation of the tensile strength and in the end Eq. [6] was applied to all the steels.

When applying Eq. [6], the values of the free C and the free N need to be known. Given that during simulated coiling a slow cooling is applied inside the furnace to reach room temperature, it can be assumed that the C equilibrium concentration is reached. Consequently, a value of 0.002 pct (room-temperature equilibrium carbon) was considered independently of the coiling temperature and of the deformation sequence. As a first approach, it was assumed there is no free nitrogen. The corresponding $\Delta\sigma_y$ values have been plotted in Figure 11, as a function of the coiling temperature and the thermomechanical sequence for the ferrite-pearlite microstructures produced in the three steels. There is some correlation between the Nb content in the steel and the level reached by $\Delta\sigma_y$, which increases with the Nb content in the steel. A decrease of the coiling temperature produces an increase in $\Delta\sigma_y$ in steel A, for both sequences. Nevertheless, S1 produces higher values than S2. But the lowest value of $\Delta\sigma_y$ (~40 MPa) is obtained for the reference test (S2-R) in which case, the model[27] predicts the complete precipitation of Nb in austenite. This precipitation was confirmed by transmission electron microscopy observations.[25] Previous estimations about the contribution of the precipitation in austenite to the yield stress in steels with similar compositions (0.07 to 0.08C; 0.68 to 1.00Mn; 0.043 to 0.065Nb) to steel A gives the reported value $\Delta\sigma_y \cong$ 65 MPa, including the effect of free C.[8,35]

C. Strengthening Contribution from Free N and Dynamic Strain Aging

The $\Delta\sigma_y$ values obtained for steel C are almost independent of the coiling temperature. The holding stage at 1143 K (870 °C) applied to steel C during the S1-R sequence gives a yield stress of 320 MPa and a tensile strength of 478 MPa, which are almost the same as for the S1 sequence. This is logical as, according to the predictions from the model[25] no precipitation is
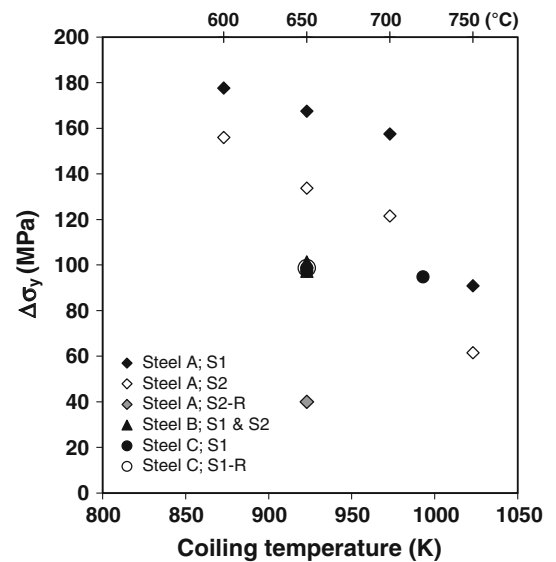

Fig. 11—Upper bound (assuming there is no free N) for the contribution of the Nb to the strengthening. (Estimations made by the application of Eq. [6].).

expected during the holding stage at 1143 K (870 °C) in this steel because of its relatively low Nb content. For steel B, the S1 and S2 pass sequences give almost the same $\Delta\sigma_y$.

A quantitative analysis of the net effect of Nb on the strength of the material requires correction for the eventual N_{ss} contribution. The maximum contribution to the yield stress from free nitrogen, according to Eq. (7), results in about 31, 39, and 20 MPa for steels A, B and C, respectively. This equation assumes a linear dependency between free nitrogen and the associated strengthening term, but a non-linear relation has also been proposed of the form $\Delta\sigma_{\mathrm{Nss}} = k_N \mathrm{N}_{ss}^{0.5}$, with k_N a constant adopting different values, depending on the source (i.e., $k_N = 354$,[4] $k_N = 425$[36]). However, for the current range of N contents, the maximum difference in predicted contribution, depending on the equation, is as low as 2 MPa. Accordingly, the following equation will be used[3]:

$$\Delta\sigma_{y\mathrm{Nb}} = \Delta\sigma_y - 5544\,\mathrm{N}_{\mathrm{free}} \qquad [8]$$

Attempts made to measure the free nitrogen by internal friction tests were unsuccessful. Alternatively, the presence of free nitrogen was assessed by performing tensile tests at different temperatures in the range where the dynamic strain aging (DSA) manifests. The presence of N in solution produces DSA in C-Mn steels, leading to an eventual increase in the tensile strength and lower ductility when deformation is performed at approximately 473 K (200 °C) instead of at room temperature.[37] For microalloyed steels, the dynamic strain aging is less intense and takes place at higher temperatures.[38]

The serrations produced by the Portevin-LeChatelier effect clearly manifest in the tensile curves shown in Figure 8. It can be observed that the elongation for the tensile tests performed at 473 K (200 °C) is higher than

that at 293 K (20 °C), but it decreases for the tests performed at a higher temperature. Coiling at 873 K (600 °C) produces a singular behavior, shown in Figure 8. For the rest of the selected conditions, the tensile strength decreases monotonously with the temperature of the tensile test in the 293 K to 623 K (20 °C to 350 °C) range. This is in line with the behavior observed for different steels grades,[39–41] particularly when the addition of strong nitride forming elements like B[39] or V[40] removes nitrogen from the solid solution. Transmission electron microscopy has revealed Nb(C,N) interphase precipitates and AlN particles at dislocations in steel A processed according to the S1 sequence and coiled at 1023 K (750 °C). The removal of N from the solution during high-temperature coiling, because of AlN precipitation, is generally accepted for C-Mn steels,[42,43] which explains the very low DSA occurring at the 1023 K to 973 K (750 °C to 700 °C) temperature range (Figure 8).

The difference, ΔTS_{DSA}, between the tensile strength at a given testing temperature and that at room temperature, produces negative values for most of the cases. The evolution of ΔTS_{DSA} as a function of the coiling temperature has been plotted in Figure 12 for two tensile test temperatures (i.e., 473 K and 623 K [200 °C and 350 °C]). The ΔTS_{DSA} curve passes through a minimum at a coiling temperature of approximately 873 K (600 °C) when the tensile tests are carried out at 200 °C (473 K). In fact, this coiling temperature divides the graph into two regions. For ferrite pearlite microstructures ($T_{coiling} \geq 873$ K [600 °C]), the absolute value of ΔTS_{DSA} decreases with increasing coiling temperature. The opposite happens when acicular or bainitic components appear in the microstructure ($T_{coiling}$ below ~873 K [600 °C]). For the lowest coiling temperature investigated, ΔTS_{DSA} becomes slightly positive. This pattern is completely modified for the tensile test performed at 623 K (350 °C). ΔTS_{DSA} is affected by the peak appearing for the coiling at 873 K (600 °C). A ferrite-pearlite microstructure together with some free nitrogen is responsible for this singular behavior obtained for coiling at 873 K (600 °C).

Transmission electron microscopy has revealed[25] that coiling at 873 K (600 °C) produces homogeneous and fine Nb-rich precipitation in ferrite. Several precipitates, from all of those analyzed by energy-dispersive X-ray spectroscopy, showed traces of Al in addition to Nb. But no AlN like those observed after S1 and coiling at 1023 K (750 °C) were observed, nor in thin foils or extraction replicas.[25] This holds with previously reported results on low-carbon Al-killed steels, indicating that the precipitation of AlN is suppressed at low coiling temperatures.[42,43] According to the current results, the presence of Nb does not significantly modify this pattern. Nevertheless, hot rolling sequences followed by direct quenching, reheating to the coiling temperature, and coiling simulation, produces the precipitation of NbN, followed by NbC formation when N has been consumed.[44,45] This finding indicates that the tempering of the martensite taking place during this type of sequence produces a different precipitation pattern than direct cooling from finishing to the coiling temperature.
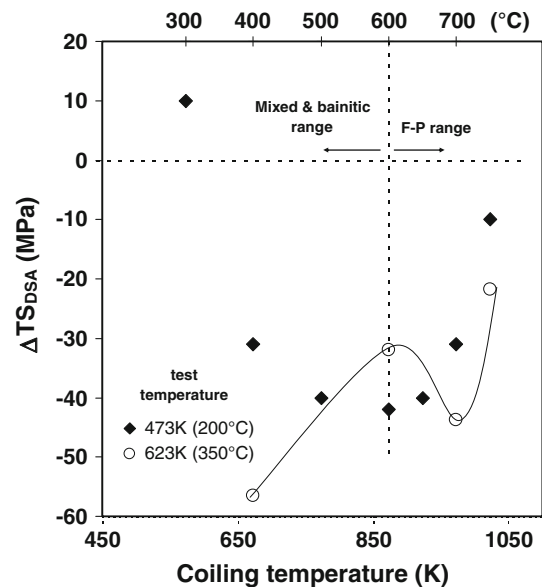

Fig. 12—Difference, because of DSA, between the tensile strength obtained from tests performed at the indicated temperature and at room temperature, as a function of the coiling temperature.

The N in solution present after coiling at 873 K (600 °C) (Figure 9) is responsible for the DSA that breaks the monotonously decreasing tendency of the tensile strength when increasing the tensile testing temperature. In C-Mn steels, the magnitude of this deviation depends on the amount of free N. Nevertheless, the peak tensile strength for S1 and coiling at 873 K (600 °C) is relatively low when compared with the one obtained for C-Mn-Mo-Nb steels of nitrogen content similar to steel A.[41] This could indicate that the amount of N in solution is low even for S1 and coiling at 873 K (600 °C) sequence. Alternatively, it is known that the precipitates finely dispersed in the matrix are effective sinks for free interstitial elements.[46] Interstitial atoms segregate to the matrix/particle interfaces if enough thermal energy for diffusion is provided. For the tests performed in the 473 K to 623 K (200 °C to 350 °C) temperature range, it can be assumed that nitrogen atmospheres segregate quickly to the NbC/ferrite interface. In this way, free nitrogen is partially removed from solution and aging reduces.

Coiling at low temperatures leads to the formation of nonpolygonal ferrite and here again the DSA is very low. Apparently, the sensitivity of bainitic microstructures to dynamic strain aging is low because of the presence of transformation dislocations.[47,48] In fact, yield point elongation on the tensile curves obtained when deforming at room temperature is clearly observed for S1 and coiling at 873 K (600 °C), but it almost disappears for the coiling at 773 K (500 °C) and is absent at lower coiling temperatures.

The concentration of free nitrogen as a function of coiling temperature was estimated for the case of a C-Mn steel via modeling,[49] and the exact contribution from the Nb, $\Delta\sigma_{yNb}$, was deduced by the application of Eq. [7]. In contrast, regarding the concentration of the Nb in solution before transformation to ferrite, Nb_{free}
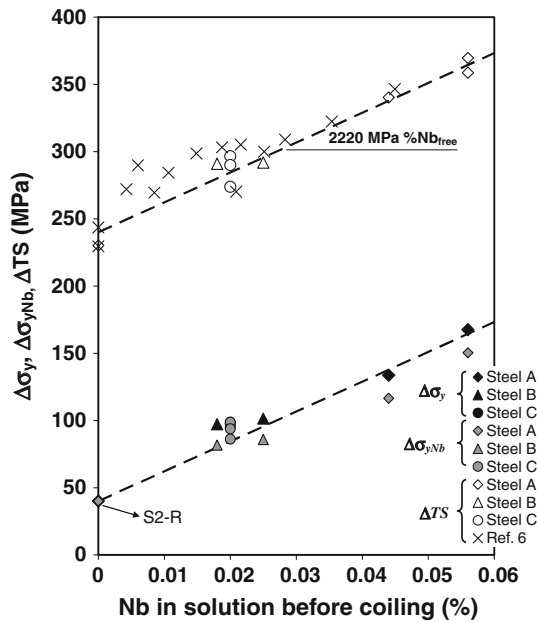
Fig. 13—Increase of the yield stress after correction for solutes, free nitrogen, and grain size effects, as a function of the estimated Nb remaining in solution before coiling at 923 K (650 °C).

Fig. 14—Estimated contribution from Nb, to the material strengthening, as a function of the coiling temperature.

was estimated from the MOFRIPE model.[27] For example, for steel A processed according to the S2 sequence, the strain-induced precipitation in austenite limits the amount of available Nb_{free} to approximately 0.044 pct, whereas for the S2-R, the model predicts the complete precipitation of Nb in austenite ($Nb_{free} \cong 0$). The values for $\Delta\sigma_y$ and $\Delta\sigma_{yNb}$ corresponding to a coiling temperature of 923 K (650 °C) have been plotted in Figure 13 as a function of the estimated Nb_{free}. The common linear relationship results for the three steels leads to

$$\Delta\sigma_y(\text{MPa}) = 40 + 2220\, Nb_{free} \qquad [9]$$

with Nb_{free} in (wt pct). When taking into consideration the N-corrected yield stress $\Delta\sigma_{yNb}$, a better fit is obtained using a smaller slope of approximately 1900 MPa per pct Nb_{free}. The increase in tensile strength from Nb has been estimated by using the same equation applied in[6]

$$\Delta TS(\text{MPa}) = TS_{exp} - 49\,\text{Mn} - 112\,\text{Si}$$
$$- 3.0\,\text{Pearlite(pct)} - 12.16 d^{-0.5} \quad [10]$$

except the coefficient affecting the pearlite term, which was 4.9 MPa per pct pearlite in the original article has been substituted here by 3 MPa per pct pearlite. This modification does not significantly affect the results obtained in Reference 6, which correspond to low-carbon steels (<0.07 pct C) or in steel A, for the same reason. These two sets of results almost superimpose when the ΔTS is plotted as a function of the estimated Nb_{free} (Figure 13). Nevertheless, the results corresponding to steels B and C, which contain a higher carbon content and therefore a larger volume fraction of pearlite (20 to 25 pct) than steel A, need the previously
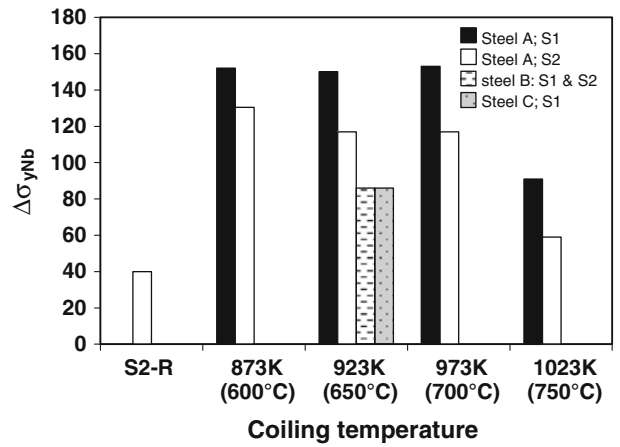
mentioned correction of the coefficient to adjust the obtained results into the same scatter band exhibited by the low-carbon steels. It must be noted that the slope proposed in Reference 6 for the ΔTS plot is the same one that applies to the $\Delta\sigma_y$ plot (Eq. [8]). The extra strengthening obtained in Reference 6 was attributed by the authors to the coherent precipitation of Nb (<3 nm size precipitates) taking place at intermediate coiling temperatures (823 K to 923 K [550 °C to 650 °C]).

The values for $\Delta\sigma_{yNb}$ obtained for the three steels have been plotted in Figure 14 as a function of the coiling temperature in the 873 K to 1023 K (600 °C to 750 °C) range. The maximum contribution is reached for steel A in agreement with its higher Nb content. The strain-induced precipitation of Nb in austenite during the S2 thermomechanical sequence reduces the Nb contribution, independently of the coiling temperatures because of the strain-induced precipitation of this element in austenite. Additionally, the net effect of Nb increases significantly when the coiling temperature decreases, which is in agreement with previous results.[6] No signs of significant difference in the dislocation density into the ferrite grains obtained after S1 and coiling at 1023 K and 873 K (750 °C and 600 °C) was detected by TEM and electron backscattered diffraction.[25] Consequently, the difference in the $\Delta\sigma_{yNb}$ values should be attributed to the effect of Nb precipitation in ferrite. Transmission electron microscopy has revealed some discontinuous interphase precipitation for S1 and coiling at 1023 K (750 °C), whereas coiling at 873 K (600 °C) produced very fine and homogeneous precipitates.[25] Given that S1 and coiling at 873 K (600 °C) presents indices of free N, these homogeneous precipitates should be of the type NbC that follow a semicoherent orientation relationship with the ferrite matrix and remain stable in size even for large holding times (48 hours) at 873 K (600 °C).[25]

The NbC precipitates in steel A coiled at 873 K (600 °C) follow a Baker-Nutting orientation relationship with the ferrite. This gives semicoherent precipitates in ferrite. For the range of NbC cubic carbides that are reported (4.43 to 4.47 nm) lattice misfits of ~43 and
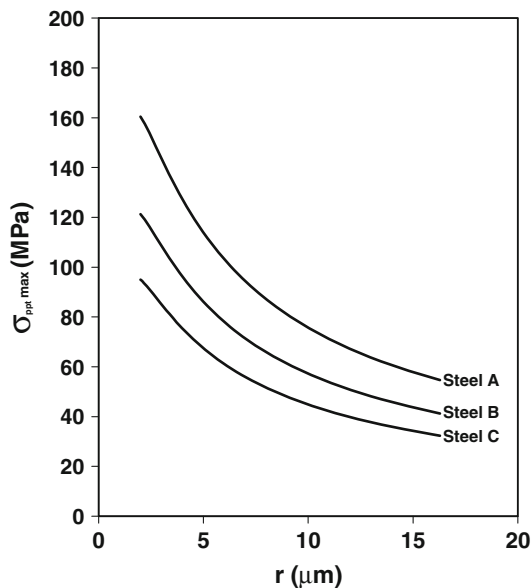
Fig. 15—Maximum expected precipitation strengthening in the different steels, according to Ashby-Orowan equation, as a function of the particle mean diameter.

9 pct are obtained for the planes pairs: $\{001\}_\alpha$ to $\{001\}_{NbC}$ and $\{001\}_\alpha$ to $\{011\}_{NbC}$, respectively. There is a general consensus about the fact that TEM images do not reveal the typical contrast observed for coherent particles. The presence in some cases of weak streaks indicates that the NbC has precipitated as platelets lying on the $\{001\}_{NbC}$ // $\{001\}_\alpha$ planes.[50] No indices of coherency contrast or of streaks were observed for the fine precipitates found in steel A,[23] and a spherical shape was assumed.

D. Precipitation Strengthening

Ashby-Orowan's equation (Eq. [5]) was applied to estimate the theoretical upper bound of the variation of precipitation contribution σ_{ppt} with the precipitate diameter, assuming that all the Nb in the steel had finely precipitated (Figure 15). The value $\Delta\sigma_{yNb} \cong \sigma_{ppt} \cong$ 90 MPa that was obtained for steel A processed according to the sequence S1 and coiling at 1023 K (750 °C) (Figure 14) can be reached for a precipitate mean diameter of about 7.5 nm (Figure 15). Transmission electron microscopy[25] revealed a mean particle size of around 6 nm in this specimen. Accordingly, Ashby-Orowan's formulation correctly predicts the extra strengthening caused by Nb.

For the sequence S1 and coiling at 873 K (600 °C), the value $\Delta\sigma_{yNb} \cong \sigma_{ppt} \cong$ 152MPa can be reached for a mean particle diameter of approximately 2.5 nm (Figure 15). Transmission electron microscopy performed on steel A after coiling at 873 K (600 °C) revealed the presence of fine precipitates homogeneously distributed in the matrix.[25] The observation of these particles required dedicated TEM work. It was not possible to obtain dark-field images of the precipitates and the measurements performed on bright-field images

obtained from thin foils overestimated their actual size.[23,24] Subsequent work on extraction replicas showed very fine precipitates in steel A when coiled at 873 K (600 °C). A microanalysis performed on the coarsest of them (~5 nm) clearly indicated that they are Nb rich.[25] It is not possible to obtain a quantitative estimation of these very fine precipitates by transmission electron microscopy. Nevertheless, extremely small particles (2.4 nm mean diameter) have already been observed by small-angle neutron scattering for coiling simulations performed at 873 K (600 °C)[51] in a Fe-Nb-C laboratory alloy containing 110 ppm C and 780 ppm Nb. Some precipitation takes place during the 65 minutes of holding at 873 K (600 °C) and continues during the subsequent cooling to room temperature, but the size of the precipitates is not significantly affected, which holds with the observed size stability of the precipitates in the current steel.[25]

Ashby-Orowan's equation loses validity for small precipitates when these are coherent and become penetrable to dislocations. For shearable precipitates, the stress increases with the particle size at a given volume fraction, until the maximum precipitation-strengthening stress is reached at the transition from shearable to nonshearable particles.[22] The question that could be raised is how shearable are the extremely fine NbC precipitates (2 to 3 nm) with a Baker-Nutting orientation relationship. But it can be concluded that, given the value of $\sigma_{ppt} \cong 152$ MPa that was deduced for S1 and coiling at 873 K (600 °C), the critical NbC particle diameter at the transition between shearable and nonshearable particle should be at approximately 2.5 nm, which is reasonable.[6] Consequently, even if considering NbC as shearable, Ashby-Orowan's equation would provide a sufficiently good estimation.

A remarkable point is the fact that, independently of the deformation sequence and of the steel composition and as long as a mixed microstructure that contains a sufficiently high fraction of polygonal ferrite is obtained, the tensile properties remain almost constant in the steel over a broad range of coiling temperatures. The fraction of acicular ferrite increases with decreasing coiling temperature, whereas the fraction of both pearlite and ferrite decrease. For a cooling rate of 5 K/s, the A_{r3} temperature in steel A was determined to be at approximately 903 K (630 °C),[52] which explains the presence of a relatively high fraction of polygonal ferrite even at low coiling temperatures.

The 15 K/s cooling rate applied to steel B from finishing to 573 K to 673 K (300 °C to 400 °C) temperature produces a fully bainitic microstructure with a yield strength of approximately 75 MPa over yield strength reached for a ferrite-pearlite microstructure (coiling at 923 K [650 °C]). It can be assumed that for the coiling at low temperatures (673 K to 573 K [400 °C to 300 °C]), the NbC precipitation in ferrite is suppressed,[6] and the extra strengthening can be mainly attributed to the microstructural refinement and to the transformation dislocations. If the estimated NbC precipitation contribution of approximately 85 MPa for S2 and coiling at 923 K (650 °C) is subtracted, and ignoring the contribution from the "grain refinement"

and extra strengthening of approximately 160 MPa, it turns out that the result can be attributed to the transition from a reconstructive type of transformation (ferrite-pearlite) to a displacive one (bainite). The application of Eq. [4], which considers isothermal transformation at 673 K (400 °C), leads to a value of approximately 260 MPa, but the transformation that takes place after S2 in steel B is anisothermal. At a cooling rate of 15 K/s, transformation starts before the 673 K (400 °C) coiling temperature is reached and results in a smaller dislocation density that that predicted by Eq. [2].

VI. CONCLUSIONS

- The processing conditions defining the thermomechanical sequence applied to condition the austenite and the coiling temperature have a significant effect on the tensile properties of the Nb microalloyed steels.
- An extra contribution to the strength (beyond the solutes and the grain size contributions) comes from the Nb remaining in solution, Nb_{free}, before transformation. The extra strengthening affecting both the yield and the tensile strength is almost proportional to the Nb_{free} and the proportionality constant is similar to previously reported values.
- The maximum extra strengthening associated with a ferrite-pearlite microstructure is obtained for a coiling temperature of 873 K (600 °C). Coiling at different temperatures below approximately 873 K (600 °C) produces mixed microstructures, but the strength remains almost stable. A cooling rate of 15 K/s to a coiling temperature of 573 K to 673 K (300 °C to 400 °C) produces a bainitic microstructure in steel B. In this case, the strength is higher than that obtained for the mixed microstructures formed when the cooling rate was 5 K/s.
- The dynamic strain aging indicates that AlN precipitation consumes the N from the solution for high coiling temperatures (1023 K [750 °C]) and for the reference tests (holding at 1143 K (870 °C), prior to coiling). However, for coiling at 873 K (600 °C), nitrogen remains in solution, leading to the usual increase of the tensile strength when the tensile test is performed in the 473 K to 623 K (200 °C to 350 °C) range. This indicates that the AlN precipitation pattern is not significantly modified by the presence of Nb in coiled specimens. Additionally, it can be concluded that the precipitation of Nb in ferrite is of the NbC type and does not consume the N. This last result is in opposition with the results obtained when normal coiling is replaced by quenching the austenite and reheating it to the coiling temperature.
- The precipitation strengthening contribution is in agreement with the predictions from Ashby-Orowan's equation.

REFERENCES

1. A.J. DeArdo: *Int. Mater. Rev.*, 2003, vol. 48, pp. 371–402.
2. C. Klikenberg, K. Hulka, and W. Bleck: *Steel Res. Int.*, 2004, vol. 75, pp. 746–54.
3. T. Gladman: *The Physical Metallurgy of Microalloyed Steels*, The Institute of Metals, London, U.K., 1997, p. 55.
4. F.B. Pickering: *Constitution and Properties of Steels, Materials Science and Engineering*, vol. 7, R.W. Cahn, P. Haasen, and E.J. Kramer, eds., Wiley VCH, Oxford, U.K., 1993, p. 47.
5. W.B. Morrison: *Proc. British Steel Corporation Conference: Controlled Processing of HSLA Steels*, British Steel Corporation, Sheffield, U.K., 1976.
6. J.C. Herman, B. Donnay, and V. Leroy: *ISIJ Int.*, 1992, vol. 32, pp. 779–85.
7. S.S. Campos, E.V. Morales, and H.J. Kestenbach: *Metall. Mater. Trans. A*, 2001, vol. 32A, pp. 1245–48.
8. T. Parigil and G. Ludkovsky: *Proc. Int. Symp. on Accelerated Cooling of Rolled Steels*, G.E. Ruddle and A.F. Crawley, eds., Pergamon Press, Oxford, U.K., 1987, pp. 131–44.
9. V. Thillou, M. Hua, C.I. Garcia, C. Perdrix, and A.J. DeArdo: *Mater. Sci. Forum*, 1998, vols. 284–286, pp. 311–18.
10. R.M. Brito and H.J. Kestenbach: *J. Mater. Sci.*, 1981, vol. 16, pp. 1257–63.
11. A. Itman, K.R. Cardoso, and H.J. Kestenbach: *Mater. Sci. Technol.*, 1997, vol. 13, pp. 49–55.
12. S.S. Campos, E.V. Morales, and H.J. Kestenbach: *Mater. Sci. Forum*, 2003, vols. 426–432, pp. 1517–22.
13. R.Z. Wang, C.I. Garcia, M. Hua, K. Cho, H.T. Zhang, and A.J. DeArdo: *ISIJ Int.*, 2006, vol. 46, pp. 1345–53.
14. R.D.K. Misra, H. Nathani, J.E. Hartmann, and F. Siciliano: *Mater. Sci. Eng. A*, 2005, vol. 394, pp. 339–52.
15. R.W. Honeycombe and G.M. Smith: *Int. Conf. Strength of Metals and Alloys (ICSMA 6)*, Pergamon Press, Melbourne, Australia, 1982, p. 407.
16. Y. Takahasi and H.K.D.H. Bhadeshia: *Mater. Sci. Technol.*, 1990, vol. 6, pp. 592–603.
17. I.D. McIvor and T.G. Gladman: BSC Research Report, PMC/6805/1/75/A.
18. S. Zajac, J. Komenda, P. Morris, P. Dierickx, S. Matera, and F. Peñalba-Diaz: *Technical Steel Research*, EUR21245EN, 2005.
19. T. Gladman: *Mater. Sci. Technol.*, 1999, vol. 15, pp. 30–36.
20. H.J. Kestenbach: *Mater. Sci. Technol.*, 1997, vol. 13, pp. 731–39.
21. A. Kelly and R.B. Nicholson: *Strengthening Methods in Crystals*, Applied Science Ltd., London, U.K., 1971.
22. B. Reppich: *Materials Science and Technology. A Comprehensive Treatment*, vol. 6, H. Mughrabi, ed., Wiley VCH, Berlin, Germany, 1993, pp. 311–57.
23. M.A. Altuna, A. Iza-Mendia, and I. Gutierrez: *3rd International Conference on Thermomechanical Processing of Steels* Padua, Italy, 2008, (CD), ed. Associazione Italiana di Metallurgia, 2008.
24. M.A. Altuna, A. Iza-Mendia, and I. Gutierrez: *Metall. Italiana*, 2009, pp. 41–47.
25. A. Iza-Mendia, M.A. Altuna, B. Pereda, and I. Gutiérrez: *Precipitation of Nb in an HSLA Steel after Austenite Conditioning. Part 1: Microstructural Analysis*, in press.
26. R.L. Higginson and C.M. Sellars: *Worked Examples in Quantitave Metallography*, Minerals and Mining The Institute of Materials, London, U.K., 2003.
27. B. López: C. Scott, A. Rose, B. Soenen, B. Lopez, and G. Paul: "Characterisation and Modelling of Strain Induced Precipitation: CAMSIP," Technical Steel Research, EUR 22431, 2006.
28. E. Cotrina, A. Iza-Mendia, B. López, and I. Gutiérrez: *Metall. Mater. Trans. A*, 2004, vols. 35A, pp. 93–102.
29. E. Novillo, E. Cotrina, A. Iza-Mendia, B. López, and I. Gutiérrez: *Mater. Sci. Forum*, 2005, vols. 500–501, pp. 355–62.
30. E. Novillo, D. Hernández, I. Gutierrez, and B. López: *Mater. Sci. Eng. A*, 2004, vol. 385A, pp. 283–90.
31. W.B. Morrison: *Trans. TMS-ASM*, 1966, vol. 59, pp. 824–46.
32. F.B. Pickering and T. Gladman: *Iron and Steel Institute*, Special Report no. 81, 1963.
33. F.B. Pickering: *Physical Metallurgy and the Design of Steels*, Applied Science Publisher Ltd., London, U.K., 1978.
34. I. Gutierrez and A. Altuna: *Acta Mater.*, 2008, vol. 56, pp. 4682–90.

35. E. Valencia and H.J. Kestenbach: *Rev. Metall. Madrid*, 1998, vol. 34, pp. 488–98.
36. T. Gladman, I.D. McIvor, and F.B. Pickering: *ISIJ Int.*, 1972, pp. 916–30.
37. C.W. Marschall, M.P. Landow, and G.M. Wilkowski: *Fracture Mechanisms: Twenty-First Symposium*, ASTM STP 1074, J.P. Gudas, J.A. Joyce, and E.M. Hackett, eds., American Society for Testing and Materials, Philadelphia, PA, 1990, pp. 339–60.
38. S. Gündüz: *Ironmaking Steelmaking*, 2002, vol. 29, pp. 341–46.
39. B.H. Cao, J.J. Jonas, P.R. Hastings, and N. Nickoletopoulos: *Mater. Sci. Forum*, 1998, vols. 284–286, pp. 543–50.
40. H. Karabulut and S. Gündüz: *Mater. Des.*, 2004, vol. 25, pp. 521–27.
41. W.R. Calado, O.J. Dos Santos, C.S.B. Castro, R.N. Barbosa, and B.M. Gonzalez: *J. Mater Sci*, 2008, vol. 43, pp. 6005–11.
42. N. Takahashi, M. Shibata, Y. Furuno, H. Hayakawa, K. Kakuta, and K. Yamamoto: *Metallurgy of Continuous Annealed Sheet Steel*, B.L. Bramfitt and P.L. Mangonon, eds., Metallurgical Society of AIME, Warrendale, PA, 1982, pp. 133–53.
43. B. Engl and E.J. Drewes: *Proc. Thechnology of Continuously Annealed Cold-Rolled Sheet Steel*, R. Pradhan, ed., The Metallurgical Society of AIME, Warrendale, PA, 1985, pp. 123–38.
44. E. Courtois, T. Epicier, and C. Scott: *Micron*, 2006, vol. 37, pp. 492–502.
45. M. Perez, E. Courtois, D. Acevedo, T. Epicier, and M. Maugis: *Phil. Mag. Lett.*, 2007, vol. 87, pp. 645–56.
46. R. Lagneborg, T. Siwecki, S. Zajac, and B. Hutchinson: *Scand. J. Metall.*, 1999, vol. 28, pp. 186–241.
47. D. Wagner, C. Prioul, and D. Francois: *J. Alloys Compd.*, 1994, vols. 211–212, pp. 132–35.
48. D. Wagner, C. Prioul, and D. Francois: *J. Nucl. Mater.*, 1998, vol. 252, pp. 257–65.
49. P.J. Evans, G.J. Spurrs, W. Hutchinson, D. Artymowicz, H.K.D.H. Bhadeshia, N. Chester, J.I. Larburu, I. Gutierrez, and J. Zaitegui: *Technical Steel Research*, EUR 19877 EN, 2001.
50. A.T. Davenport, L.C. Brossard, and R.E. Miner: *JOM*, 1997, vol. 27, pp. 21–27.
51. F. Perrard: Ph.D. Dissertation, Institut National Polytechnique de Grenoble, 2004.
52. N. Isasti: Ph.D. in course, University of Navarra.